U. S. DEPARTMENT OF COMMERCE
NATIONAL OCEANIC AND ATMOSPHERIC ADMINISTRATION
NATIONAL WEATHER SERVICE

TECHNICAL NOTE

PERFORMANCE OF TECHNIQUES USED TO DERIVE OCEAN SURFACE WINDS

WILLIAM H. GEMMILL, TSANN W. YU,
AND DAVID M. FEIT

APRIL 1987

OPC Contribution No. 14
NMC Office Note No. 330

OPC CONTRIBUTIONS

No. 1. Burroughs, L. D., 1986: Development of Forecast Guidance for Santa Ana Conditions. National Weather Digest. (in press)

No. 2. Richardson, W. S., D. J. Schwab, Y. Y. Chao, and D. M. Wright, 1986: Lake Erie Wave Height Forecasts Generated by Empirical and Dynamical Methods -- Comparison and Verification. Ocean Products Center Technical Note, 23pp.

No. 3. Auer, S. J., 1986: Determination of Errors in LFM Forecasts Surface Lows Over the Northwest Atlantic Ocean. Ocean Products Center Technical Note/NMC Office Note No. 313, 17pp.

No. 4. Rao, D. B., S. D. Steenrod, and B. V. Sanchez, 1987: A Method of Calculating the Total Flow from A Given Sea Surface Topography. NASA Technical Memorandum 87799., 19pp.

No. 5. Feit, D. M., 1986: Compendium of Marine Meteorological and Oceanographic Products of the Ocean Products Center. NOAA Technical Memorandum NWS NMC 68, 98pp.

No. 6. Auer, S. J., 1986: A Comparison of the LFM, Spectral, and ECMWF Numerical Model Forecasts of Deepening Oceanic Cyclones During One Cool Season. Ocean Products Center Technical Note/NMC Office Note No. 312, 20pp.

No. 7. Burroughs, L. D., 1986: Development of Open Fog Forecasting Regions. Ocean Products Center Technical Note/NMC Office Note. No. 323., 36pp.

No. 8. Yu, T., 1986: A Technique of Deducing Wind Direction from Altimeter Wind Speed Measurements. Mon. Wea. Rev. (Submitted).

No. 9. Auer, S. J., 1986: A 5-Year Climatological Survey of the Gulf Stream and Its Associated Ring Movements. Journal of Geophysical Research. (Submitted).

No. 10. Chao, Y. Y., 1987: Forecasting Wave Conditions Affected by Currents and Bottom Topography. Ocean Products Center Technical Note, 11pp.

No. 11. Esteva, D. C., 1987: The Editing and Averaging of Altimeter Wave and Wind Data. Ocean Products Center Technical Note, 4pp.

No. 12. Feit, D. M., 1987: Forecasting Superstructure Icing for Alaskan Waters. National Weather Digest. (Submitted).

No. 13. Rao, D. B., B. V. Sanchez, S. D. Steenrod, 1986: Tidal Estimation in the Atlantic and Indian Oceans. Marine Geodesy, 309-350pp.

TABLE OF CONTENTS

Abstract

I. Introduction

II. Description of Techniques
A. Geostrophic wind
B. Simple law
C. NMC 1000 mb wind
D. Ekman slab model
1) Linear solution
2) Non-linear solution
E. Marine boundary layer model of Cardone
F. Marine boundary layer model of Clarke and Hess
H. Summary comments concerning the techniques

III. Winds from Analyses and Forecasts Models

IV. Sources of Validation Data

A. Ship weather reports
B. Buoy reports

V. Statistical Procedures

VI. Discussion

VII. Summary

VIII. References

Abstract

Various techniques used to derive analyses and forecasts of ocean surface winds were compared. These techniques are the geostrophic relation, a simple law, an Ekman slab model, NMC forecast model 1000 mb winds, the Cardone (1969) model winds, the Clarke and Hess (1975) model winds, and the marine winds from Fleet Numerical Ocean Oceanographic Command (FNOC). Statistical comparisons of model winds with those from ships and buoys were made for wind speed, wind direction and the vector wind. The statistics suggest that none of the techniques was clearly better. The study did indicate that model wind speeds and inflow angles compare better with buoy data than ship data. For high wind speeds (>22.5 m/s) observed by ships, all models were too low. Overall, the Cardone model appears to produce slightly better verification results when both the analyses and 24 hour forecasts are compared with observations from the buoys.

1) Introduction

Over the past 30 years, advances in operational numerical weather prediction have significantly improved the ability to forecast the large scale synoptic features of the atmosphere. However, because of computer limitations and time constraints within the operational environment, numerical weather prediction models must compromise horizontal and vertical resolutions, and details of physics in order to produce timely predictions. Such atmospheric variables as wind, temperature and moisture are computed at the midpoint of the model layers and boundary layer physics is parameterized so that depiction of the detailed structure of the atmospheric boundary layer is not possible. In order to obtain these variables at the sea surface, it is necessary to apply further considerations of boundary layer physics.

In practice, operational forecasts of surface variables are made using statistical regression techniques which relate the model forecast parameters to surface weather observations (Burroughs, 1982). In order to apply the statistical approach, a continuous record of accurate observations at "fixed" weather stations is required. The resulting forecasts include the influence of local effects, as well as corrections for systematic forecast model errors. Unfortunately, the number of oceanic "fixed" observation platforms with sufficiently long records is limited and confined mostly to ocean regions near the continents.

In order to develop oceanographic and marine guidance products which provide forecasts of ocean waves, ice movement, upwelling, ocean mixing, fog, vessel icing and boundary layer clouds, it is necessary to have accurate forecasts of, among other parameters, ocean surface wind speed and direction. This report compares observed ocean surface winds with those derived from 1) large scale meteorological model fields using "diagnostic" methods, 2) NMC (National Meteorological Center) 1000 mb winds, and 3) FNOC (Fleet Numerical Oceanographic Center) marine winds.

The term "diagnostic" is used here to catagorize those methods which relate information from the large scale meteorological analyses and forecasts to ocean surface wind speed and direction. These techniques can be considered indirect approaches and are based on physical theories which assume a steady state wind, and empirical relationships. Further, they are applied grid point by grid point, with no one grid point influencing any other.

The different models evaluated were A) the geostrophic wind, B) a simple wind law (Larson, 1975), C) NMC 1000 mb winds, D) an Ekman slab model, E) Boundary layer model of Cardone (1969), F) boundary layer model of Clarke and Hess (1975), and G) FNOC winds (Mihok and Kaitala, 1976). A brief discussion of these wind models is given below. A summary is presented in Table 1.

II) Description of Techniques

A. Geostrophic Wind

Sea level geostrophic winds were determined from the gridded analyses and forecasts of sea level pressure and temperature using the standard relations:

$$Ug = -(RT/fp)(\partial p/\partial y) \qquad \text{A.1.a}$$

$$Vg = (RT/fp)(\partial p/\partial x) \qquad \text{A.1.b}$$

$$G = (Ug^2 + Vg^2)^{1/2} \qquad \text{A.2}$$

where: Ug = x-component of the geostrophic wind,
Vg = y-component of the geostrophic wind,
G = geostrophic wind speed,
and: R = universal gas constant,
T = temperature(K),
f = coriolis parameter,
p = sea level pressure.

B. Simple Law

Operational forecasters commonly determine ocean surface winds by simply reducing the geostrophic wind speed by a constant factor and rotating the direction towards low pressure by a constant angle. Larson (1975) proposed a slightly more complex formulation in his study of time series of marine winds. The reduction factor is allowed to vary as a function of latitude and the cross-isobaric angle (or inflow angle) of the wind is permitted to vary as a function of wind speed and latitude.

The appropriate equations are:

$$B = 0.6045 + 0.186(\theta/25) \quad \text{for } \theta < 25 \qquad \text{B.1.a}$$

$$B = 0.7905 \quad 25 \leq \theta < 45 \qquad \text{B.1.b}$$

$$B = 0.6975 + 0.093*(90-\theta)/45 \quad 45 \leq \theta \qquad \text{B.1.c}$$

where: B = wind reduction factor,
θ = latitude

Table 1. Ocean Surface Wind Techniques

Model	Method	Theory
Geostrophic	Geostrophic Wind	Geostrophy
Simple Law	Geostrophic Wind *Simple wind speed reduction *Simple wind direction turning	Empirical
1000 MB	Spectral Model Winds Forecasts *OI Analyses	OI, Model
Analytic	NMC's Sea Level Pressure Gradient Corrected by: *Bulk formulation for friction	Slab model
Cardone(1969,1978) Clarke & Hess (1975) FNOC (1976)	Geostrophic Wind Corrected by: * Air-Sea temperature difference * Thermal wind * Friction	Two-Region Boundary Layer Constant Flux Ekman Dynamics

and the surface wind speed is given by:

$$V_s = B * G \qquad \text{B.2}$$

where: G = geostrophic wind,

and the inflow angle (α) is given by the relation:

$$\alpha = (1.475/(1+\sin\theta))(22.5 - 0.0175V_s^2) \qquad \text{B.3}$$

C) NMC Model 1000 mb winds

Analyses of 1000 mb winds were obtained from the NMC global data assimilation system (Dey and Morone, 1985). The system provides analyses of meteorological variables; height, temperature, winds and moisture using both conventional station observations taken on the synoptic periods (00z, 06z, 12z, and 18z), and synoptic data from aircraft, satellite, etc. The analyses are made every six hours using a two step procedure. A six hour forecast is made, which is used as a first guess for the analysis. Current data are then used to update the first guess by applying multi-variate three-dimensional optimum interpolation on isobaric surfaces. Over the ocean, both surface wind and pressure observations are used to produce the 1000 mb wind analysis. In contrast, over the land surface wind observations are not used.

Forecasts of the 1000 mb winds were obtained from the NMC Medium Range Forecast model which was run once per day during the 00Z operational cycle (Sela, 1982). The initial analysis is obtained from the global data assimilation system. This model has 18 equal layers, each 28 mb thick (Since October 1986, unequal sigma levels have been incorporated into the model, with the lowest layer having a thickness of 11 mb). The boundary layer physics is the GFDL E-physics (Miyakoda and Sirutis, 1983). The 1000 mb winds were obtained from the forecast model sigma coordinate system by interpolation. Figure 1 illustrates a schematic of the model levels in relation to the mandatory observational level.

D) Ekman Slab Method

Ocean winds may be derived using a simple boundary layer slab model. The equations of motion, assuming steady state conditions may be written:

$$u\,\partial u/\partial x + v\,\partial u/\partial y - fv = -\alpha\partial p/\partial x - \partial(\overline{u'w'})/\partial z \qquad \text{D.1.a}$$

$$u\,\partial v/\partial x + v\,\partial v/\partial y + fu = -\alpha\,\partial p/\partial y - \partial(\overline{v'w'})/\partial z \qquad \text{D.1.b}$$

Figure 1. Vertical distribution of model layers, mandatory levels, and parameters. P* is the surface pressure, and S0, S1, etc., are the successive sigma levels.

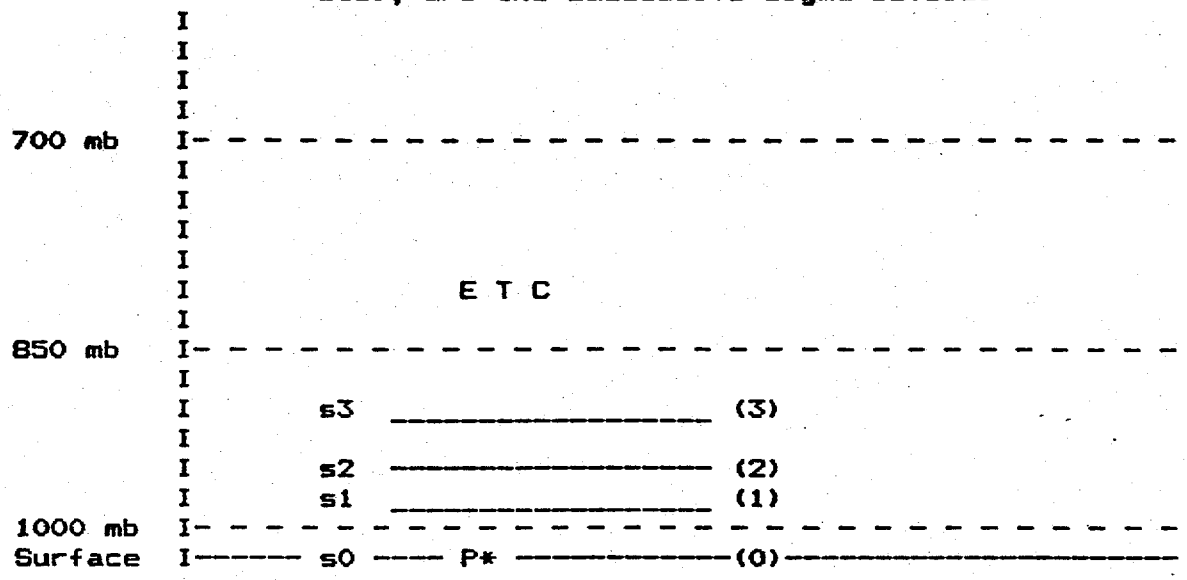

If one parameterizes the momentum fluxes ($\overline{u'w'}$), ($\overline{v'w'}$) at the ocean surface in terms of u and v and the pressure gradient at the surface is given, then the above non-linear equations are solved as a system of two equations with two unknowns through an iterative process for u and v.

(1) Linear Solution

The linear system expresses a balance between the pressure gradient, coriolis, and friction forces in the atmospheric boundary layer. The boundary layer is assumed to be a slab of constant depth (h). The momentum fluxes at the ocean surface are parameterized by a bulk transfer formula with a drag coefficient (CD) and the balance of forces may be expressed as:

$$-\alpha\,\partial p/\partial x + fv - (CD/h)\,|S|u = 0 \qquad \text{D.2.a}$$

$$-\alpha\,\partial p/\partial y - fu - (CD/h)\,|S|v = 0 \qquad \text{D.2.b}$$

In the above equations, it was assumed that the stress at the top of the boundary layer (at z=h) is zero. Through algebraic manipulation, D.2.a and D.2.b can be combined to give a fourth order equation for (S):

$$CD'^{2}S^{4} + f^{2}S^{2} - \alpha^{2}((\partial p/\partial x)^{2} + (\partial p/\partial y)^{2}) = 0 \qquad \text{D.3}$$

where: $S^{2} = u^{2} + v^{2}$ and $CD' = CD/h = 2.0 \times 10^{-6}$.

The solution for S is given by:

$$S = (-f^{2} + [f^{4} + 4CD'^{2}\alpha^{2}(\partial p/\partial x^{2} + \partial p/\partial y^{2})]^{1/2})^{1/2}/(\sqrt{2}\,CD') \qquad \text{D.4}$$

Thus, from equation D.4, one can calculate wind speed, given the pressure gradient, coriolis parameter and the frictional drag coefficient. Once S is calculated, substitution into the original equations enables u and v to be determined.

(2) Non-linear Solution

The surface wind speed and direction were also determined by adding the non-linear (advective) terms to the above linear Ekman solution. Equations D.2.a and D.2.b are now written to include the non-linear terms.

$$fv - \alpha\,\partial p/\partial x - CD'Su = u\,\partial u/\partial x + v\,\partial u/\partial y \qquad \text{D.5.a}$$

$$-fu - \alpha\,\partial p/\partial y - CD'Sv = u\,\partial v/\partial x + v\,\partial v/\partial y \qquad \text{D.5.b}$$

The non-linear equations can be solved iteratively as follows:

$$\left[CD'S^{n} + \partial u/\partial x \right] u^{n+1} - \left[f - \partial u/\partial y \right] v^{n+1} = -\alpha \partial p/\partial x \qquad D.6.a$$

$$\left[f + \partial u/\partial y \right] u^{n+1} + \left[CD'S^{n} + \partial v/\partial y \right] v^{n+1} = -\alpha \partial p/\partial y \qquad D.6.b$$

The equations can now be solved for u and v, where the index n+1 and n are the new and old values respectively. To start the iteration procedure, the linear solution is used. The nonlinear solutions are considered to converge when the following conditions are met:

$$\left| u^{n+1} - u^{n} \right| < e \quad \text{and} \quad \left| v^{n+1} - v^{n} \right| < e \qquad D.7$$

Where e, the convergence factor, is set to be 0.01 m/s for this model. In general, convergence is achieved in less than 10 iterations, except near the tropics where Coriolis parameter f becomes small and more iterations are required. Note that both linear and nonlinear equations have non-singular solutions at the equator (where f=0) under this formulation.

E) Marine Boundary Layer Model of Cardone

This model and the model that follows are similar in that they treat the atmospheric boundary layer as two vertical regimes, and include stability effects and baroclinic effects for application over the ocean. It has been shown that over the ocean the baroclinic effect (vertical wind shear) can be just as important as the stability effect (Nicholls and Reading, 1979). Both models determine the surface friction velocity (U_*) and inflow angle (α) from the surface geostrophic wind, air-sea temperature difference and the thermal wind obtained from the large scale numerical model. However, the mathematical approach of the two model is different.

Cardone developed (1969, 1978) a baroclinic, stability dependent, marine boundary layer model to specify ocean surface winds. The model separates the atmospheric boundary layer into a constant flux layer at the surface, and an Ekman layer above. At the internal boundary between the two regions, the model requires that wind speed and direction, vertical wind stress are continuous. The governing equations, for the barotropic case, are derived based on the equations for each region with the appropriate surface, internal and free atmosphere boundary conditions, and are written:

$$U_* = G \left[2KB \sin^{2}(\alpha) / \phi(h/L') \right]^{1/3} \qquad E.1.a$$

$$U_* = \sqrt{2}\, GK \sin(\pi/4 - \alpha) / \left[\ln(h/z_o) - \psi(h/L') \right] \qquad E.1.b$$

where: U_* = friction velocity,
α = inflow angle,
G = geostrophic wind,

K = von Karman's constant (0.4),
ψ = stability function,
ϕ = non-dimensional wind shear,
z_o = roughness length,
L' = modified Monin length,
h = depth of constant flux layer,
B_o = 0.0003, proportional constant for height of constant flux layer.

The modified Monin length is given as:

$$L' = U_*^2 Ta[\ln(z/z_o) - \psi(z/L')]/[K^2 g(Ta - Ts)] \qquad E.2$$

where:
Ta = air temperature (K)
Ts = sea surface temperature (K)
z = height of air temperature
g = gravity

The height of the constant flux layer is assumed proportional to G/f and is expressed as:

$$h = B_o G/f \qquad E.3$$

where:
f = coriolis parameter

The roughness length is formulated as:

$$z = (0.684/U_*) + 4.38\ 10^{-5} U_*^2 - 4.43\ 10^{-2} \qquad E.4$$

Equations E.1.a, E.1.b, E.2, E.3 and E.5 now represent a complete set of equations which can be used to determine the friction velocity (U_*) and the inflow angle (α), if the correct relations for the non-dimensional wind shear (ϕ) and stability function (ψ) are known.

The stability correction function (ψ) is mathematically related to the non-dimensional wind shear (ϕ) by the following integral:

$$\psi(z/L') = \int_{(z_o/L')}^{(z/L')} \frac{[\,1 - \phi(\zeta)\,]}{\zeta}\, d\zeta \qquad E.5$$

where the form of the function (ϕ) is given by:

$$\phi = 1 + B'\, z/L', \qquad B'=7 \text{ (stable)} \qquad E.6.a$$

$$\phi = 1, \qquad \text{(neutral)} \qquad E.6.b$$

$$\phi^4 - (Y'\, z/L')\,\phi^3 - 1 = 0, \qquad Y'=17 \text{ (unstable)} \qquad E.6.c$$

Given U_*, z_o and $\psi(z/L')$, the wind can now be specified at height z, within the constant layer, which for this study is at 10 m, and is given by:

$$U(z) = (U_*/K)[\ln(z/z_o) - \psi(z/L')] \qquad E.8$$

There are three parameters that are important to this boundary layer model, but whose relationships must be empirically determined from field measurement studies. These parameters are the stability dependent non-dimensional wind shear (ϕ), the surface roughness (z_o) as a function of surface stress, and the scaling factor (B_o) for the height of the internal boundary layer.

For the full baroclinic case, equations E.1.a and E.1.b are reformulated with the inclusion of the non-dimensional wind shear (thermal wind) parameter:

$$|dG/dz|/f \qquad E.9$$

and the angle between the wind shear vector and the surface geostrophic wind. In this case the equations become more complex and can be found in Cardone(1969).

F) Marine Boundary Layer Model of Clarke and Hess

Clarke and Hess (1975) have also developed a marine boundary model, based on similarity theory, which incorporates baroclinic and stability effects. The atmospheric boundary layer is assumed to be divided into two distinct regions, the inner layer (which is about 50 m thick), and the outer region which extends to the top of the boundary which is 1-2 km. The inner layer is a constant flux layer and the outer layer is the Ekman layer. The equations for the two layers along with the boundary conditions are similar to the Cardone model. However, the mathematical basis of this technique is the asymptotic matching of wind from the constant flux layer to the Ekman layer across the interior height h, through dynamic similarity scaling arguments. This approach provides equations that link the "external" parameters of the free atmosphere such as geostrophic wind, thermal wind, and air-sea temperature difference to the "internal" parameters of surface stress and inflow angle, without direct knowledge of internal boundary height and the top of the boundary layer.

The Rossby number similarity theory is applied to the governing atmospheric equations, which are written:

$$K\,U_g'/U_* = \ln(U_*/fz_o) - A \qquad F.1.a$$

$$K\,V_g'/U_* = -B|f|/f \qquad F.1.b$$

where: U_g' = component of geostrophic wind in the direction of U

V_g' = component of geostrophic wind 90 degrees to the left of U
U_* = friction velocity
f = coriolis parameter
z_o = roughness length
K = von Karman's constant (0.4)
A, B = similarity functions

By combining equations F.1.a and F.1.b with some algebraic manipulation, a new equation, F.2.a, is obtained. Further, equation F.1.b can be rewritten, using the trigonometric relation

$$V_g' = G \sin(\alpha),$$

to obtain equation F.2.b. The inflow angle (α) is the directional difference between the geostrophic wind and surface stress. Equations F.2.a and F.2.b can be solved for the two unknowns of friction velocity (U_*), and inflow angle (α) given the geostrophic wind speed and stability. The height of the internal boundary is not a required variable in the solution.

$$\ln(R_o) = A - \ln(U_*/G) + (K^2G^2/U_*^2 - B^2)^{1/2} \qquad \text{F.2.a}$$

$$\alpha = \sin^{-1}(BU_*/KG) \qquad \text{F.2.b}$$

where the Rossby number is defined as:

$$R_o = G/(fz_o) \qquad \text{F.3}$$

the roughness length is specified as:

$$z_o = 0.016\, U_*^2/g \qquad \text{F.4}$$

where g = gravity

and G = geostrophic wind speed

The similarity functions A, B are dependent upon stability. Extensive field experiments and research has been conducted to determine these universal functions. Clarke and Hess (1975) modified the Rossby number similarity theory to include the baroclinic effect and also to include the ocean surface current as a function of friction velocity. Equations F.1.a and F.1.b are rewritten as:

$$K(U_g' - U_s')/U_* = \ln(U_*/(fz_o) - A(\varphi,s) \qquad \text{F.5.a}$$

$$K(V_g' - V_s')/U_* = -B(\varphi,s)|f|/f \qquad \text{F.5.b}$$

where the sea surface current is specified to be the friction velocity (U_*) and its relative components are:

$$U_s' = U_* \cos(\alpha) \qquad \text{F.6.a}$$

$$V_s' = U_* \sin(\alpha) \qquad \text{F.6.b}$$

Again combining the U and V components of the Rossby number similarity theory equation and after some algebraic manipulations, U_* and α can be determined from the two equations that follow:

$$\ln(R_o) - A(\mu,s) - \ln(G/U_*) - [K^2(G/U_* - 1)^2 - B^2(\mu,s)]^{1/2} = 0 \qquad \text{F.7}$$

$$\alpha = \sin [B(\mu,s)/((K(G/U_* - 1))] \qquad \text{F.8}$$

where the stability parameter is given by:

$$\mu = gK^2(Ta - Ts) / (fGTa) \qquad \text{F.9}$$

Ta = air temperature (K)
Ts = sea surface temperature (K)

and the baroclinic parameters are given by:

$$s = (sx^2 + sy^2)^{1/2} \qquad \text{F.10}$$

$$sx = (K^2/f)\,\partial u_g'/\partial z, \qquad \text{F.11.a}$$

$$sy = (K^2/f)\,\partial v_g'/\partial z \qquad \text{F.11.b}$$

The similarity functions $A(\mu,s)$ and $B(\mu,s)$ have been derived as:

$$A(\mu,s) = A(\mu) + A(s) + A_0 \qquad \text{F.12.a}$$

$$B(\mu,s) = B(\mu) + B(s) + B_0 \qquad \text{F.12.b}$$

where $A_0 = 1.1$ and $B_0 = 4.3$ are the neutral barotropic values for A and B. $A(\mu)$ and $B(\mu)$ are the contributions due to stability. A(s) and B(s) are the contributions due to the baroclinic effect. Clarke and Hess used the following relations:

$$A(\ ) = -0.10\mu - 0.001\mu^2 \qquad \text{F.13.a}$$

$$B(\ ) = 0.13\mu - 0.001\mu^2 \qquad \text{F.13.b}$$

$$A(s) = 0.20sx - 0.04sy \qquad \text{F.14.a}$$

$$A(s) = -0.32sx + 0.35sy \qquad \text{F.14.b}$$

G) FNOC Marine Winds

Unlike the NMC's 1000 mb winds which are analyzed on fixed isobaric surfaces using optimum interpolation analysis, the FNOC winds are analyzed at the ocean surface using a variational analysis method (Mihok and Kaitala, 1976, and L. Clark (FNOC), 1986 personal communication). Forecast winds are derived from output from the NOGAPS model.

H) Summary comments concerning the models

The techniques that were evaluated have been presented in order of complexity. These techniques are "diagnostic" models, which determine ocean surface winds from the large scale atmospheric analyses and forecasts. The simplest method for obtaining ocean surface winds is to directly calculate the geostrophic wind. However, it is well known the actual surface winds are less than geostrophic and are turned toward lower pressure. The Simple Law is based on empirical equations which provide the surface wind speed and direction from the geostrophic wind. This technique will produce the general pattern of the large scale wind field.

However, the simple empirical law is just that, a simple empirical adjustment to the geostrophic wind. Theoretical models provide a logical framework to progress from the simple to the complex with an orderly physical interpretation. The one-layer slab model was designed on the premise that simple Ekman theory could be used to deduce surface winds, given the sea level pressure analysis. This technique was formulated to be well behaved at the equator unlike the geostrophic wind relation. A deficiency of this slab model, is the use of a constant drag coefficient. Although, the diabatic and baroclinic effects were not included in the model, it was extended to include the non-linear advection terms. However, inclusion of the nonlinear terms in this formulation did not appreciably improve the ocean surface winds.

The next level of complexity treats the atmospheric boundary layer as two regions and includes stability and baroclinic effects. In this study, two representative models were evaluated; one which determines the surface stress and surface inflow angle based on a system of equations for each region with boundary conditions at the ocean surface, top of the constant flux layer, and top of the boundary layer (Cardone), and the other that determines the surface stress and inflow angle using the appropriate equations and boundary conditions based on dynamic similarity scaling theory (Clarke and Hess). Because a boundary layer theory does not present closed set of equations, the Cardone model requires empirical knowledge of the non-dimensional wind shear function ϕ and height of the internal boundary layer (through the constant B_0), and Clarke and Hess require knowledge of the similarity functions A and B. Both models require functional relation between the surface stress and the surface roughness. It has been shown by Krishna (1981) that if the equations from two layer analytical model are written in the form of similarity equations (for barotropic case), the similarity functions can be expressed in terms of B_0 , ϕ and ψ . Krishna scaled the internal boundary height on U_*/f rather than G/f, which results in the constant B_1 instead of B_0. The similarity functions have been determined from extensive field experiments in order to determine empirical relations for a range of stability and

$$V_s' = U_* \sin(\alpha) \qquad \text{F.6.b}$$

Again combining the U and V components of the Rossby number similarity theory equation and after some algebraic manipulations, U_* and α can be determined from the two equations that follow:

$$\ln(R_o) - A(\mu,s) - \ln(G/U_*) - [K^2(G/U_* - 1)^2 - B^2(\mu,s)]^{1/2} = 0 \qquad \text{F.7}$$

$$\alpha = \sin [B(\mu,s)/((K(G/U_* - 1))] \qquad \text{F.8}$$

where the stability parameter is given by:

$$\mu = gK^2(Ta - Ts) / (fGTa) \qquad \text{F.9}$$

Ta = air temperature (K)
Ts = sea surface temperature (K)

and the baroclinic parameters are given by:

$$s = (sx^2 + sy^2)^{1/2} \qquad \text{F.10}$$

$$sx = (K^2/f)\,\partial U_g'/\partial z, \qquad \text{F.11.a}$$

$$sy = (K^2/f)\,\partial v_g'/\partial z \qquad \text{F.11.b}$$

The similarity functions $A(\mu,s)$ and $B(\mu,s)$ have been derived as:

$$A(\mu,s) = A(\mu) + A(s) + A_0 \qquad \text{F.12.a}$$

$$B(\mu,s) = B(\mu) + B(s) + B_0 \qquad \text{F.12.b}$$

where $A_0 = 1.1$ and $B_0 = 4.3$ are the neutral barotropic values for A and B. $A(\mu)$ and $B(\mu)$ are the contributions due to stability. A(s) and B(s) are the contributions due to the baroclinic effect. Clarke and Hess used the following relations;

$$A(\,) = -0.10\mu - 0.001\mu^2 \qquad \text{F.13.a}$$

$$B(\,) = 0.13\mu - 0.001\mu^2 \qquad \text{F.13.b}$$

$$A(s) = 0.20sx - 0.04sy \qquad \text{F.14.a}$$

$$A(s) = -0.32sx + 0.35sy \qquad \text{F.14.b}$$

G) FNOC Marine Winds

Unlike the NMC's 1000 mb winds which are analyzed on fixed isobaric surfaces using optimum interpolation analysis, the FNOC winds are analyzed at the ocean surface using a variational analysis method (Mihok and Kaitala, 1976, and L. Clark (FNOC), 1986 personal communication). Forecast winds are derived from output from the NOGAPS model.

H) Summary comments concerning the models

The techniques that were evaluated have been presented in order of complexity. These techniques are "diagnostic" models, which determine ocean surface winds from the large scale atmospheric analyses and forecasts. The simplest method for obtaining ocean surface winds is to directly calculate the geostrophic wind. However, it is well known the actual surface winds are less than geostrophic and are turned toward lower pressure. The Simple Law is based on empirical equations which provide the surface wind speed and direction from the geostrophic wind. This technique will produce the general pattern of the large scale wind field.

However, the simple empirical law is just that, a simple empirical adjustment to the geostrophic wind. Theoretical models provide a logical framework to progress from the simple to the complex with an orderly physical interpretation. The one-layer slab model was designed on the premise that simple Ekman theory could be used to deduce surface winds, given the sea level pressure analysis. This technique was formulated to be well behaved at the equator unlike the geostrophic wind relation. A deficiency of this slab model, is the use of a constant drag coefficient. Although, the diabatic and baroclinic effects were not included in the model, it was extended to include the non-linear advection terms. However, inclusion of the nonlinear terms in this formulation did not appreciably improve the ocean surface winds.

The next level of complexity treats the atmospheric boundary layer as two regions and includes stability and baroclinic effects. In this study, two representative models were evaluated; one which determines the surface stress and surface inflow angle based on a system of equations for each region with boundary conditions at the ocean surface, top of the constant flux layer, and top of the boundary layer (Cardone), and the other that determines the surface stress and inflow angle using the appropriate equations and boundary conditions based on dynamic similarity scaling theory (Clarke and Hess). Because a boundary layer theory does not present closed set of equations, the Cardone model requires empirical knowledge of the non-dimensional wind shear function Φ and height of the internal boundary layer (through the constant B_0), and Clarke and Hess require knowledge of the similarity functions A and B. Both models require functional relation between the surface stress and the surface roughness. It has been shown by Krishna (1981) that if the equations from two layer analytical model are written in the form of similarity equations (for barotropic case), the similarity functions can be expressed in terms of B_0, Φ and Ψ. Krishna scaled the internal boundary height on U_*/f rather than G/f, which results in the constant B_i instead of B_0. The similarity functions have been determined from extensive field experiments in order to determine empirical relations for a range of stability and

thermal wind conditions. Both two-layer analytic models and similarity theory models have been used in numerical prediction. However, while the similarity theory does not require the height of the internal boundary layer, it is not as straight forward to include more complex physics as in the two layer analytic models.

III) Winds from Analysis and Forecast Models

The wind models were run daily for 0000 UTC from December 3, 1985 through January 6, 1986 to generate wind fields on a 2.5 by 2.5 latitude/longitude grid for analyses (meteorological variables obtained from the NMC global data assimilation system) and 24 hour forecasts (obtained from the NMC spectral atmospheric forecast model). The comparison study covers 35 days of early winter conditions. During that period, 28 days of FNOC winds were available for comparison. Observations were matched, with interpolated model winds, for analyses and forecasts.

The data distribution for the 35 day period of reports taken at 0000 UTC and received over the GTS for the areas used in the study are shown in Figure 2. The location of the data buoys used in the study are presented in Figure 3. The typical global distribution of ship reports taken at the synoptic hour of 0000 UTC on 12 December 1985 is shown in figure 4. It is evident that the coverage of surface data is insufficient for providing an adequate analysis for many regions over the ocean.

IV) Sources of Validation Data

A. Ship Weather Reports

Two types of observations were used as standards to measure the accuracy of the models - ship weather reports and data obtained from the NWS fixed buoy network.

Meteorological observations from ships at sea are prepared by deck officers as part of their routine duties. The observations are recorded in a weather log and transmitted to coastal receiving stations via radio in an internationally agreed upon World Meteorological Organization (WMO) code. This code consists of up to 20 weather parameter groups one of which contains a report of wind speed and direction. These reports are disseminated world wide in real time via the Global Telecommunications System (GTS).

Wind speed and direction are estimated either indirectly by the observer using the sea state and the feel of the wind or directly by anemometer if the vessel is so equipped. Based upon data compiled by Earle (1985) for the period 1980-1983 46% of ship reports in the Pacific and 44% of Atlantic ship reports were from vessels without anemometers. Dischel and Pierson (1986) discuss the characteristics of wind observations made with and without anemometers. They note that errors from anemometer

Figure 2. Ship data distribution for investigation period, December 3, 1985 through January 6, 1986 for 00Z. Coastal reports (less than 50 km from land) were excluded. Data were received via the GTS.

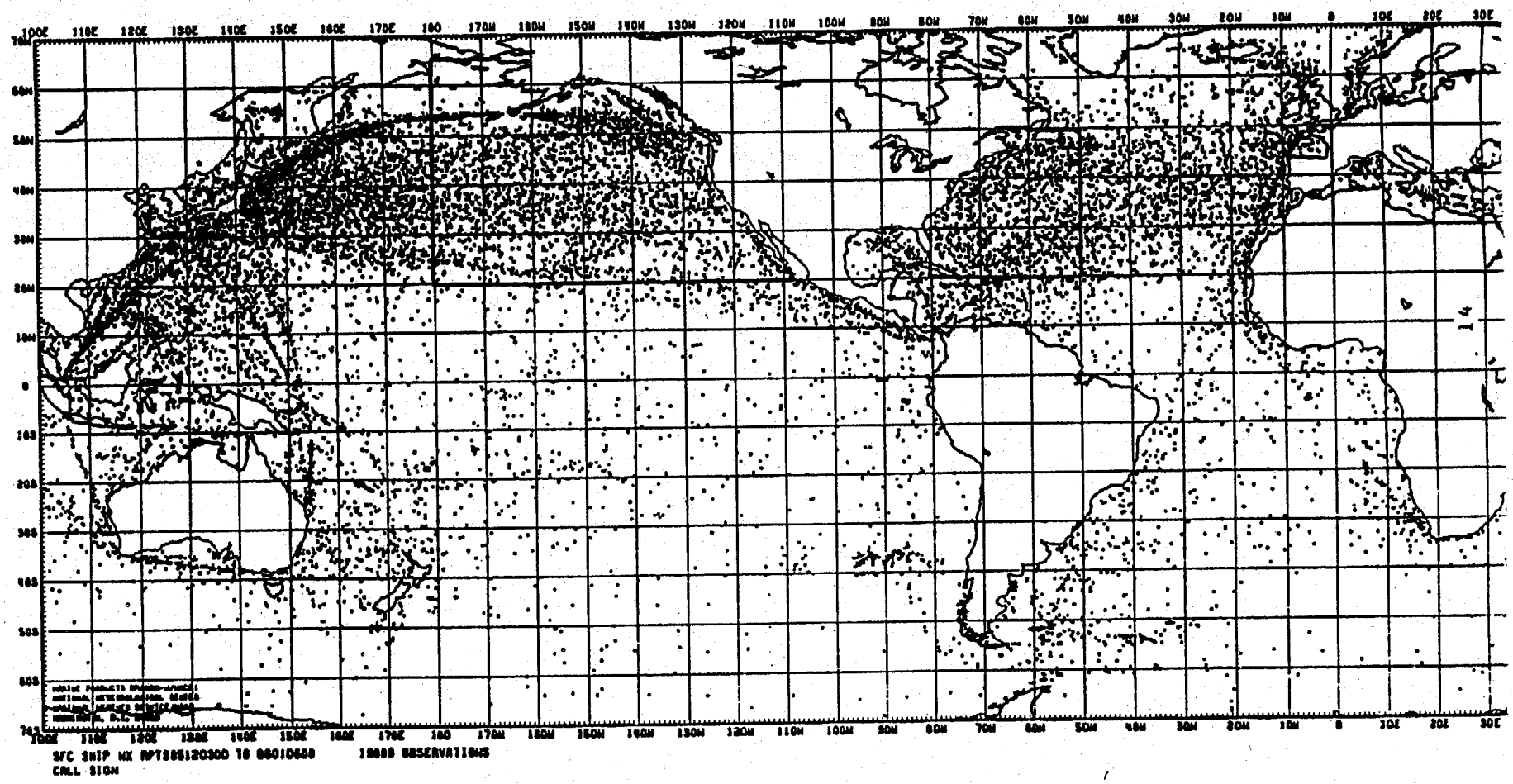

Figure 3. Location of fixed buoys.
Coastal buoys were excluded.

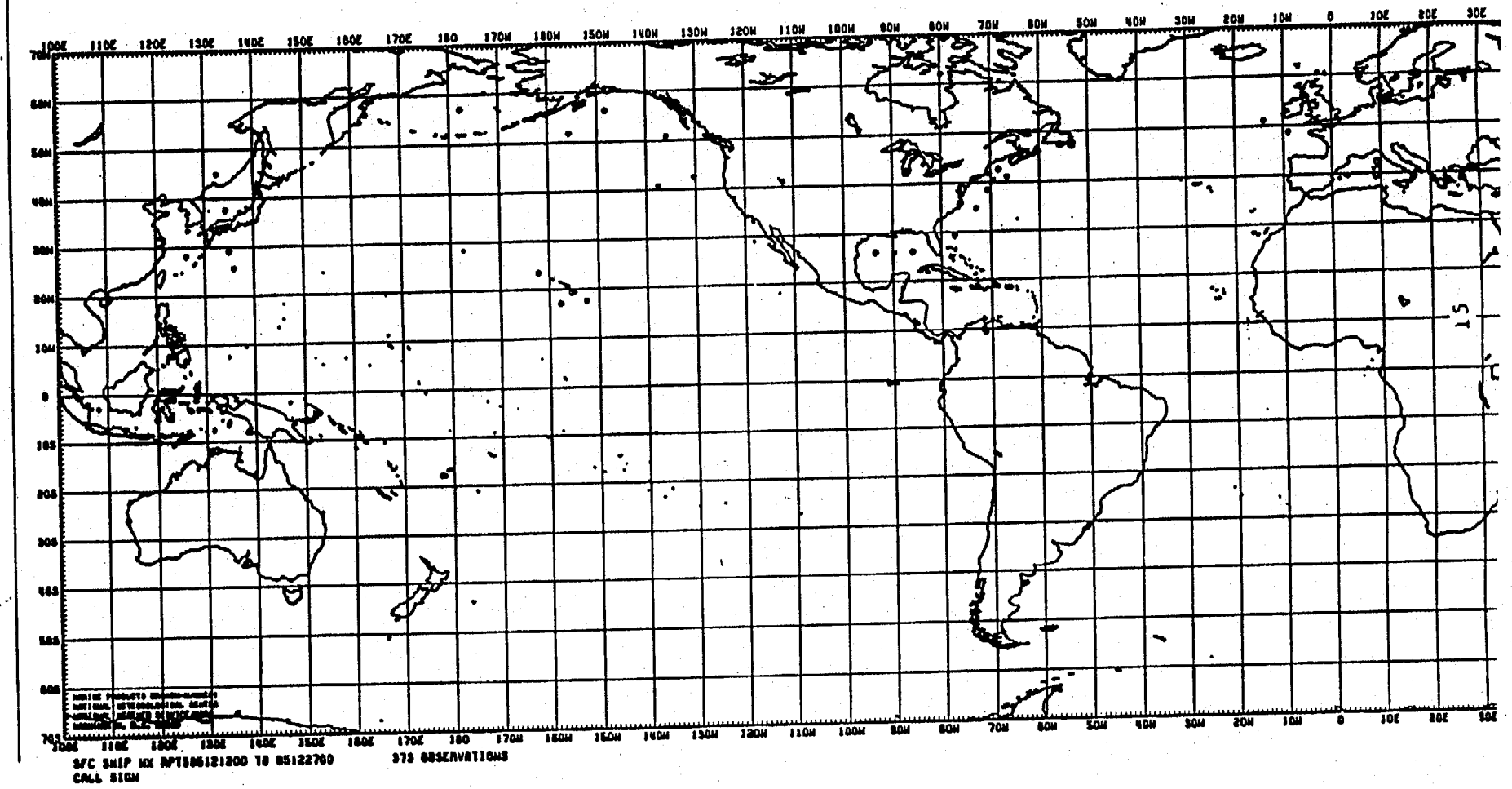

Figure 4. Distribution for all wind reports
for one synoptic period, 00Z, December 12, 1985.

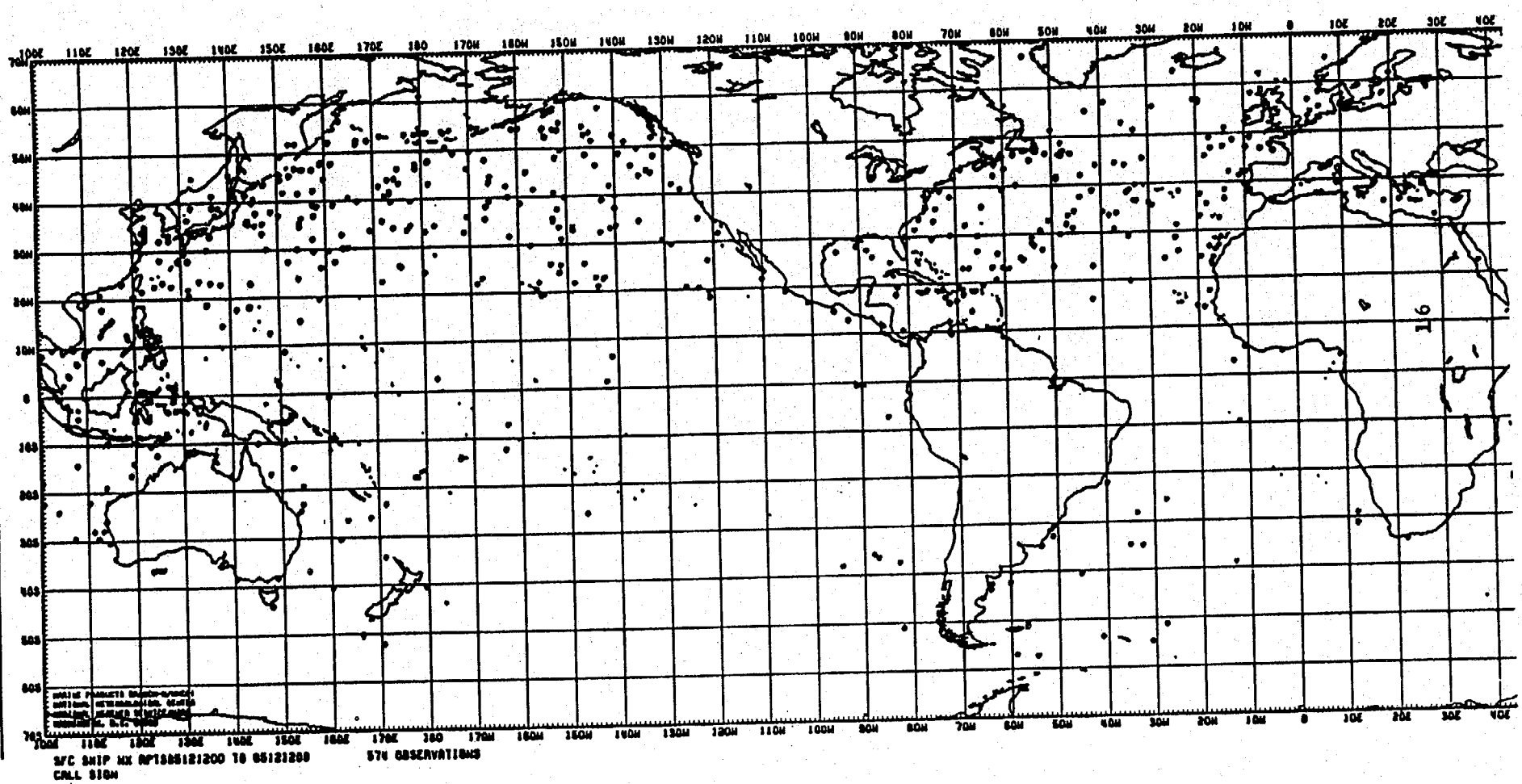

measurements can be introduced by poor instrument exposure, improper reading of the wind speed and direction indicators, and vessel motion. In addition wind instruments exposed to severe marine meteorological conditions can lose their calibration.

Estimated wind observations are also subject to a wide variety of errors. Such reports are often made by the observer by first determining the wind speed parameter in terms of the Beaufort scale where each scale number represents a range of possible wind speeds. From this a single speed is chosen for reporting purposes. Furthermore the scale is based, for the most part, on the appearance of the state of the sea. However, it is well known that there may be a substantial time lag for the sea to reach a state that truly reflects the concurrent wind force conditions. In addition, it is obvious that night time wind reports based upon visual sea state observations are subject to great error.

Ship wind observations were collected from reports transmitted over the GTS, which have been processed at NMC with only minimal quality control error checking. There is no distinction made between whether the report is estimated or measured. Further, for measured winds there is no correction for varying anemometer heights.

B. Fixed Buoy Reports

Since 1967 moored buoys, equipped with meteorological instruments, have provided surface atmospheric and oceanographic data for marine use. Buoys can be expected to provide improved data compared to that reported by ships for several reasons. First, each sensor location is carefully considered to avoid exposure problems. Second, measurement sampling frequencies and averaging periods are determined after accounting for buoy motion. Third, duplicate sensors are used and each is calibrated before deployment. Finally, all data are monitored in near real time to detect instrument errors. Gilhousen (1986) reported that the buoys are presently providing measurements which are within the original accuracy specifications. Table 2 (National Climatc Data Center, 1983) shows the specified buoy system accuracy for wind speed and direction.

Table 2

	Reporting Range	Sampling Interval	Averaging Period	Total System Accuracy
Speed	0 - 155kt	1 sec	8.5 min	SD +/- 1.9 kt or 10%
Direction	0 - 360 deg	1 sec	8.5 min	Sd +/- 10 deg

Remark: Sensor heights vary between 5 and 10 meters above the water.

V) Statistical Procedures

The statistical comparisons are made for wind speed, wind direction and vector wind, for both analyses and 24 hour forecasts with ship and buoy data.

Because wind direction is a circular function (0 - 360 degrees), standard statistical methods for linear data sets can not be used directly. For instance, Turner (1986) has discussed several methods to determine the standard deviation of wind direction as well as its mean direction. In this paper, wind direction statistics were determined relative to the cross isobaric angle (inflow angle toward lower pressure), in order to eliminate the cross over problem of wind direction at 360°. The evaluation of inflow angle is important because of its relation to low level convergence.

Standard statistical measures were used in order to compare and evaluate the models with observations. Willmott (1982) has discussed the use of difference measures in order to evaluate model performance, and states that no one measure can be expected to provide satisfactory information. In this study we used a similar set of statistical difference measures. However, wind is a vector so that standard scalar measures are not complete, and additional vector statistical measures have been included.

The measures used for this study are given by the following definitions:

Wind speed:

Correlation coefficient:

$$\left(N\sum S_o S_m - \sum S_o \sum S_m\right) \Big/ \left[N\sum S_o^2 - \left(\sum S_o\right)^2\right]^{1/2} \left[N\sum S_m^2 - \left(\sum S_m\right)^2\right]^{1/2} \qquad S.1$$

Average absolute difference:

$$\sum |S_o - S_m| / N \qquad S.2$$

Average algebraic difference:

$$\sum (S_o - S_m) / N \qquad S.3$$

and the Root mean square difference:

$$\left[\sum (S_o - S_m)^2 / N\right] \qquad S.4$$

where S_o = observed wind speed

Sm = model wind speed,
N = number of comparisons

Wind direction:

Average inflow angle:

$$\sum(\alpha_o - \alpha_g)/N \qquad S.5$$

Average absolute difference:

$$\sum|\alpha_o - \alpha_m|/N \qquad S.6$$

Average algebraic difference:

$$\sum(\alpha_o - \alpha_m)/N \qquad S.7$$

and the Root mean square difference:

$$\left[\sum(\alpha_o - \alpha_m)^2/N\right]^{1/2} \qquad S.8$$

where g = direction of the isobars with low pressure to the left (direction of the geostrophic wind),
o = direction of the observed wind, and
m = direction of the model wind.

Vector wind:

Average vector wind difference

$$\sum[(u_o-u_m)^2 + (v_o-v_m)^2]^{1/2}/N \qquad S.9$$

Root Mean Square vector wind difference:

$$\left(\sum[(u_o-u_m)^2 + (v_o-v_m)^2]/N\right)^{1/2} \qquad S.10$$

A wind vector correlation coefficient was calculated using the formulation developed by Court (1958). In the formulation, the correlation between two sets of wind vectors, W1 and W2, can be determined by a combination of expressions containing the scalar wind components. The wind vector W1 is composed of a component (u1) toward the east and (v1) toward the north, and the wind vector W2 is composed of a component (u2) toward the east and (v2) toward the north. The following expression has been used to determine the wind vector correlation coefficient ($R_{W_1W_2}$):

$$R_{W_1W_2} = \{[S^2_{v1}(S^2_{u1u2} + S^2_{v1u2}) + S^2_{u1}(S^2_{u1v2} + S^2_{v1v2}) - 2S_{u2v2}(S_{u1u2}S_{u1v2} + S_{v1u2}S_{v1v2})] / [(S^2_{u1} + S^2_{v1})(S^2_{u2}S^2_{v2} - S^2_{u2v2})]\} \qquad S.11.$$

The relations for the wind vector correlation are of the form:

$$S^2_{u1} = \sum(u1 - \overline{u1})^2/N \;,\quad S_{u1v2} = \sum(u1 - \overline{u1})(v2 - \overline{v2})/N$$

VI) Discussion

Wind speed data distributions (number of observations and percent) at 1m/sec intervals are presented in Table 3. The mean wind speed for ship data was 10.1 m/sec, with a standard deviation of 5.4 m/sec, and for buoy data the mean was 7.4 m/sec with a standard deviation of 3.4 m/sec. The mean wind speed data and and the wind speed distribution data indicated that major storm activity did not affect the regions of the fixed buoys, but that ships, whose routes cover a much wider part of the ocean did encounter some major storm activity. But, it was also suspected that high wind speeds may be overestimated by observers on ship. Ships reporting high wind speeds were subjectively compared with the Northern Hemisphere Surface Analysis to determine whether the reports were reasonable or not. It was found that some of the high wind speeds were obviously erroneous (i. e. not supported by the synoptic pattern), but others were located in frontal zones, squalls, or within intense cyclonic systems which may be reasonable but can not be resolved by the large scale model. Those wind reports that were identified as erroneous have been eliminated from the evaluation.

Comparisons of model winds with observations are presented in Tables 4 through 9, for wind speed, wind direction and vector wind, for both analyses and 24 hour forecasts. The tables separate the data by type, ship and buoy; and by region, northern hemisphere (> 17 N), east coast (25N to 50N, the coast out to 55W), and west coast (20N to 65N, 180W to the coast). The regions are identified in Figure 2. Tables 10 and 11 show the average algebraic difference and RMS difference as a function of wind speed. The data used to produce these tables do not include reports within 50km of land or data over lakes. Wind speed data were rejected when the geostrophic wind and model wind differed by more than 40kts, and wind direction data when the model direction differed from observation by more than 105 degrees for analyses (165 degrees for 24 hour forecasts).

Inspection of the tables indicates the no one model is superior to the others in all respects. However, a few general comments can be made concerning the statistics. The models verify better against the buoys than ships. This is not unexpected. Reports from fixed buoys are closely monitored and quality controlled in order to provide reliable data (Gilhousen, 1986), whereas the quality of ship reports has been shown to be questionable (Dischell and Pierson, 1986, and Earle, 1985). Hence, the following discussion will be primarily concerned with comparing the model winds with buoys. Another point to be made is that the models verify better with the east coast buoys than with the west coast. This possibly reflects a poorer quality analysis over the Northeast Pacific compared with the Northwest Atlantic.

Source	Calm	>0	>1	2	3	4	5	6	7	8	9
Ships	151	17	198	435	513	770	919	1081	1106	1324	1107
(%)	1.1	0.1	1.4	3.1	3.7	5.6	6.6	7.8	8.0	9.6	8.0
Buoys	14	3	22	33	47	56	95	112	99	145	77
(%)	1.6	0.3	2.5	3.8	5.4	6.5	10.9	12.9	11.4	16.7	8.9

Source	10	11	12	13	14	15	16	17	18	19
Ships	1049	769	943	626	479	659	180	322	346	218
(%)	7.6	5.6	6.8	4.5	3.4	4.6	1.3	2.3	2.5	1.6
Buoys	48	35	40	18	7	6	1	4	3	2
(%)	5.5	4.8	4.6	2.1	0.8	0.7	0.1	0.5	0.3	0.2

Source	20	21	22	23	24	25	26	27	28	29
Ships	224	85	69	95	46	36	28	19	14	16
(%)	1.6	0.6	0.5	0.7	0.3	0.3	0.2	0.1	0.1	0.1
Buoys	0	0	1	–	–	–	–	–	–	–
(%)	0	0	0.1							

Source	30	31	32	33	34	35	36	37	38	39
Ships	10	6	4	0	1	3	0	1	0	0
(%)	0.1	<0.1	<0.1	0	<0.1	<0.1	0	<0.1	0	0

Table 3. Data distribution by ships and buoys at intervals of 1 m/s such that the wind speed is the truncated speed, for example 5 is the range 5 to <6 m/s, 6 is 6 to < 7 m/s, and so forth. Mean wind speed for ships is 10.1 m/s with standard deviation of 5.4 m/s. Mean wind speed for buoys is 7.4 m/s with standard deviation of 3.4 m/s.

MODEL		Correlation			Ave. Abs. Diff.			Ave. Alg. Diff.			RMSD		
		NH	WC	EC	NH	WC	EC	NH	WC	EC	NH	WC	EC
Geostrophic	Ship	.66	.71	.71	3.8	4.0	3.4	-0.9	-1.7	0.6	5.0	5.2	4.5
	Buoy	.70	.77	.79	3.5	4.9	2.7	-2.3	-4.3	-1.6	4.6	6.1	3.5
Simple Law	Ship	.66	.71	.71	3.4	3.2	3.7	-1.4	0.9	2.5	4.5	4.2	4.8
	Buoy	.71	.77	.79	2.4	2.9	2.0	0.2	1.8	0.3	3.1	3.7	2.5
1000 mb	Ship	.68	.72	.74	3.4	3.5	3.4	-0.6	-1.4	-0.0	4.5	4.6	4.0
	Buoy	.71	.77	.78	3.1	4.0	2.5	-2.1	-3.6	-1.5	4.0	5.0	3.2
Yu	Ship	.63	.68	.67	3.5	3.4	3.4	-0.1	-0.6	-1.3	4.6	4.5	4.4
	Buoy	.68	.73	.78	3.0	3.8	2.4	-1.8	-3.2	-1.2	3.8	4.8	3.0
Cardone	Ship	.61	.63	.68	3.7	3.6	3.9	-2.1	2.0	2.9	4.8	4.7	5.1
	Buoy	.67	.70	.75	2.5	2.4	2.2	0.2	-0.6	0.1	3.2	3.2	2.9
Clarke/Hess	Ship	.65	.70	.73	3,3	3.0	3.4	0.9	-0.6	1.6	4.3	4.0	4.1
	Buoy	.67	.77	.77	2.5	3.1	1.9	-0.6	-2.3	-0.6	3.2	3.9	2.5
FNOC	Ship	.69	.72	.75	3.1	3.0	2.9	0.5	-0.0	1.6	4.1	4.0	4.0
	Buoy	.74	.75	.82	2.3	3.1	1.8	-0.9	-2.3	-0.5	3.2	4.2	2.6

Table 4. Ships/Buoys vs Models (Analyses) Comparisons for Wind Speed (m/sec). NH: Northern hemisphere > 17N, WC: West Coast and EC: East Coast

MODEL		Correlation			Ave. Abs. Diff.			Ave. Alg. Diff.			RMSD		
		NH	WC	EC	NH	WC	EC	NH	WC	EC	NH	WC	EC
Geostrophic	Ship	.59	.61	.68	4.2	4.6	3.7	-1.0	-1.7	0.0	5.5	5.9	4.9
	Buoy	.61	.66	.70	3.9	4.9	4.0	-2.5	-4.0	-2.8	5.1	6.3	5.3
Simple Law	Ship	.59	.60	.68	3.8	3,8	3.7	1.4	0.9	2.1	4.9	5.0	4.0
	Buoy	.61	.66	.70	2.9	3.3	2.8	-0.3	-1.6	-0.7	3.7	4.2	3.5
1000 mb	Ship	.58	.59	.68	3.6	3.9	3,3	0.0	-0.6	0.2	4.8	5.1	4.4
	Buoy	.60	.64	.67	3.3	4.2	3.4	-2.1	-3.2	-2.6	4.3	5.3	4.5
Yu	Ship	.56	.59	.65	3.8	4.0	3.5	-0.2	-0.6	0.9	5.0	5.2	4.6
	Buoy	.59	.64	.70	3.5	4.0	3.2	-1.9	-3.0	-2.0	4.4	5.0	4.0
Cardone	Ship	.60	.61	.70	3.8	3.7	3.7	+2.2	2.1	2.5	4.9	4.9	4.8
	Buoy	.65	.68	.79	2.6	2.5	2.4	0.3	-0.3	-0.6	3.3	3.1	3.0
Clarke/Hess	Ship	.59	.62	.70	3.6	3.5	3.4	1.3	1.0	0.9	4.7	4.9	4.4
	Buoy	.60	.68	.70	2.6	2.8	2.6	-0.4	-1.4	-1.1	3.4	3.6	3.2
FNOC	Ship	.52	.53	.52	3.8	3.8	4.2	1.3	1.0	2.2	4.9	4.9	5.4
	Buoy	.45	.51	.41	3.1	3.3	3.3	-.3	-1.4	-0.2	3.9	4.1	3.9

Table 5. Ships/Buoys vs Models (24 hour forecasts) Comparisons for Wind Speed (m/sec).

MODEL		Inflow Angle			Ave. Abs. Diff.			Ave. Alg. Diff.			RMSD		
		NH	WC	ECI	NH	WC	ECI	NH	WC	ECI	NH	WC	ECI
Geostrophic	Ship	0	0	0	30	27	32	*21	16	24	37	34	39
	Buoy	0	0	0	31	24	36	*24	17	34	38	31	42
Simple Law	Ship	19	18	19	23	22	24	2	-2	5	31	30	32
	Buoy	19	17	19	22	18	23	5	0	14	30	26	29
1000 mb	Ship	17	13	21	21	21	24	4	3	3	29	29	32
	Buoy	20	12	28	19	17	17	4	5	6	27	25	22
Yu	Ship	17	17	15	23	22	24	4	-1	9	31	30	32
	Buoy	16	15	13	23	19	25	8	2	20	31	27	32
Cardone	Ship	16	14	16	23	22	24	5	2	8	30	30	24
	Buoy	18	14	19	21	18	21	6	3	15	29	26	26
Clarke/Hess	Ship	19	19	18	23	22	24	2	-3	6	31	30	32
	Buoy	22	19	21	21	19	17	2	-2	14	29	26	24
FNOC	Ship	20	17	19	21	20	21	1	-1	5	29	29	31
	Buoy	21	17	22	18	16	17	3	0	12	26	23	24

Table 6. Ships/Buoys vs Models (Analyses) Comparisons for Wind Direction (Degrees). The computed inflow angles between observation direction and geostrophic direction is presented as the statistic under average algebraic difference for the geostrophic model.

MODEL		Inflow Angle			Ave. Abs. Diff.			Ave. Alg. Diff.			RMSD		
		NH	WC	ECI	NH	WC	ECI	NH	WC	ECI	NH	WC	ECI
Geostrophic	Ship	0	0	0	37	37	35	17	15	18	49	50	45
	Buoy	0	0	0	35	33	32	18	11	26	45	45	38
Simple Law	Ship	19	17	19	32	34	29	-2	2	-1	46	47	42
	Buoy	19	17	19	28	31	21	-1	-6	8	40	44	29
1000 mb	Ship	21	15	16	32	33	30	-4	0	2	46	48	42
	Buoy	21	12	23	28	31	21	-3	-1	3	40	44	29
Yu	Ship	17	17	16	33	34	30	0	-2	2	46	48	42
	Buoy	16	14	15	28	31	22	2	-3	12	40	43	30
Cardone	Ship	15	15	16	32	34	29	2	0	2	46	47	41
	Buoy	18	15	18	28	30	20	1	-4	8	40	44	28
Clarke/Hess	Ship	19	20	17	32	33	29	-2	-5	1	45	48	41
	Buoy	21	22	19	28	31	21	-3	-11	7	41	45	28
FNOC	Ship	14	15	9	37	38	40	3	0	9	52	54	54
	Buoy	12	11	7	40	37	43	6	0	19	55	53	59

Table 7. Ships/Buoys vs Models (24 hour forecasts) Comparisons for Wind Directions (Degrees).

MODEL		Vector Correlation			Vect. Err. Magn.			Vect. Err. RMS		
		NH	WC	ECI	NH	WC	ECI	NH	WC	ECI
Geostrophic	Ship	.72	.75	.70	7.4	7.3	7.0	9.1	9.0	8.7
	Buoy	.73	.82	.79	6.4	6.1	6.2	7.7	7.8	7.5
Simple Law	Ship	.72	.74	.68	5.7	5.5	5.8	7.2	7.0	7.3
	Buoy	.74	.83	.80	4.4	4.2	4.1	5.5	5.0	4.8
1000 mb	Ship	.76	.77	.73	5.8	5.9	5.4	7.4	7.5	7.1
	Buoy	.79	.84	.83	4.7	5.3	3.9	5.8	6.1	4.6
Yu	Ship	.72	.74	.69	6.1	6.0	5.8	7.6	7.5	7.4
	Buoy	.74	.81	.80	5.2	5.3	4.7	6.3	6.1	5.5
Cardone	Ship	.70	.72	.67	5.8	5.6	5.7	7.1	7.0	7.1
	Buoy	.73	.81	.79	4.2	3.7	3.8	5.3	4.4	4.6
Clarke/Hess	Ship	.72	.74	.70	5.7	5.6	5.5	7.2	7.1	7.0
	Buoy	.74	.82	.80	4.4	4.5	3.6	5.5	5.3	4.2
FNOC	Ship	.75	.76	.72	5.3	5.2	5.0	6.9	6.9	6.8
	Buoy	.78	.84	.85	3.9	4.3	3.3	5.3	5.3	4.3

Table 8. Ships/Buoys vs Models (Analyses) Comparisons for Wind Vector (m/sec).

MODEL		Vector Correlation			Vect. Err. Magn.			Vect. Err. RMS		
		NH	WC	ECI	NH	WC	ECI	NH	WC	ECI
Geostrophic	Ship	.65	.62	.64	8.1	8.6	7.4	9.8	0.5	9.2
	Buoy	.69	.71	.78	6.8	7.3	6.5	8.1	8.7	7.9
Simple Law	Ship	.64	.61	.62	6.7	7.0	6.3	8.2	8.7	7.9
	Buoy	.69	.71	.79	5.0	5.4	4.3	6.1	6.3	5.1
1000 mb	Ship	.66	.62	.65	6.8	7.4	6.3	8.4	9.1	8.0
	Buoy	.70	.70	.78	5.6	6.4	5.1	6.8	7.4	6.0
Yu	Ship	.65	.62	.62	7.1	7.4	6.4	8.6	9.1	8.1
	Buoy	.69	.70	.79	5.8	6.2	4.9	6.9	7.2	5.6
Cardone	Ship	.64	.61	.62	6.5	6.7	6.1	7.9	8.2	7.7
	Buoy	.69	.71	.80	4.6	4.5	3.8	5.6	5.4	4.4
Clarke/Hess	Ship	.64	.62	.63	6.5	6.8	6.1	8.0	8.4	7.8
	Buoy	.69	.72	.78	4.9	5.0	4.1	5.9	5.9	4.7
FNOC	Ship	.60	.59	.49	7.1	7.3	7.5	8.6	8.9	8.9
	Buoy	.59	.62	.62	5.9	5.9	6.0	6.9	6.8	6.7

Table 9. Ships/Buoys vs Models (24 hour forecasts) Comparisons for Wind Vector (m/sec).

In order to compare the change in performance of the models from analyses to 24 hour forecasts, an additional statistical measure was defined: the Average of the RMS Differences (ARMSD) from all the models (except geostrophic) for the northern hemispheric buoys for analyses and for forecasts.

Comparisons of the analyses of model wind speeds with buoys (Table 4) shows that the geostrophic wind speeds are too high by 2.3 m/s, and have an RMS difference of 4.6 m/s. But, the 1000 mb wind speeds are also high by 2.1 m/s with an RMS difference of 4.0 m/s. The diagnostic models reduce the wind speed in agreement with theory, as the average bias of the models (excluding the geostrophic) was reduced to 0.8 m/s too high and the ARMSD was 3.4 m/s. The model performance statistics do not indicate which of the models is best.

When comparing the 24 hour wind speed forecasts with buoys (Table 5), the model performances show a slight deterioration, the ARMSD increases from 3.4 m/s for analyses to 3.8 m/s for forecasts. Cardone's model has a slight statistical edge for forecasts, it's RMS difference was lowest at 3.3 m/s.

The inflow angle of the buoy wind direction is computed relative to the geostrophic wind direction and is given by the average algebraic difference of the geostrophic wind (Table 6). The inflow angle is found to be twice as large for the east coast as for the west coast. Air masses along the west coast have had a long trajectory over the ocean and are near neutrally stable conditions, whereas along the east coast cold air masses from the continent move eastward over the warmer coastal and Gulf Stream waters producing an unstable boundary layer, and as theory predicts, a larger inflow angle.

Comparison of the wind directions indicate that there is little difference between models (Tables 6 & 7). Again, the geostrophic wind does the poorest when compared with the buoys with an RMS difference of 38 degrees, whereas the ARMSD was 29 degrees. However, along the east coast the 1000 mb winds were closest (average algebraic difference was smallest) to the buoy wind directions. The tendency of the models is not to turn the winds enough, especially when large inflow angles are computed. The 24 hour forecast ARMSD for wind direction increased to 43 degrees, with FNOC wind direction RMS difference was greatest at 55 degrees. Again the best wind direction forecasts were along the east coast where the average RMS difference was about 30 degrees (excluding FNOC winds and geostrophic winds).

These statistics point out several problems concerning the evaluation of inflow angle from the models. Inflow angles are on the order of 10 to 30 degrees which is small when compared with the natural variability of the wind and errors in its reported measurement. Wind directions are reported to the nearest 10 degrees and the fixed buoy sensor accuracy is $\pm$ 10 degrees. Thus, although the absolute wind direction can be determined reasonably accurately, the inflow angle correction is small when compared with

the uncertainty of the wind direction measurement. Therefore, it is difficult to differentiate model performance on the basis of inflow angle.

The comparison of the wind vector statistics (Tables 8 & 9) lead to a similar conclusion about the wind models as noted above. Analyses of geostrophic winds exhibit the largest vector differences when compared with buoys (RMS difference was 7.7 m/s), whereas the ARMSD was 5.6 m/s. For 24 hour forecasts the vector error RMS was 8.1 m/s for geostrophic winds, and the ARMSD was 6.3 m/s. Cardone wind forecasts were slightly better (vector RMS difference is 5.6 m/s which is lowest) than the other models. The average vector RMS difference of the models along the east coast also indicates more accurate forecasts of wind direction (5.4 m/s).

Tables 10 and 11 are presented to identify model performance in terms of bias and RMS as a function of wind speed. At high wind speeds (above 15 m/s) the mean model wind speeds begin to deviate from the mean buoy wind speeds, with Cardone under specifying the wind the most. Although, at speeds above 22.5 m/s there were no buoy speeds for comparison, ship speeds are much larger than the model wind speed. The large-scale models seem to be incapable of specifying the high wind speeds. The discrepancy between models and observations at high wind speed is related to the coarse resolution (2.5 x 2.5 degrees) of the analyses and forecast fields on one hand and the tendency for observers to over estimate high winds, on the other.

VII) Summary

A study has been made to compare various techniques for deriving wind fields at the ocean surface. Over the past 20 years a number of approaches have been proposed, based on application of boundary layer physics. Table 1 presents a brief summary of the techniques reviewed and investigated in this study. Although statistics were included for both ship and buoy data, it was evident that only buoy data were suitable for use as "ground truth" for the comparisons. This conclusion has been, also, has been reported by several recent studies.

It was found that the model wind speeds verify better with buoy data than ship data, and verify better with east coast buoys than west coast buoys. Comparisons of wind direction indicates that the accuracy of models are about the same (except for the geostrophic case which is clearly the poorest). The inflow angle is small relative to the variability and measurement of wind direction.

This study showed that for northern hemispheric analyses, the wind models, when compared with buoys, were able to specify wind speed with an ARMSD of 3.4 m/s, wind direction of 29 degrees and vectors with 5.6 m/s. The 24 hour forecast RMS differences for wind speed were 3.8 m/s, for wind direction were 43 degrees, for wind vector 6.3 m/s.

MODEL		Algebraic difference					
		0-45	0-5	5-10	10-15	15-22.5	22.5-30	30-45
Geostrophic	Ship	-0.9	-2.6	-1.3	-0.7	0.4	3.8	16.1
	Buoy	-2.3	-2.0	-2.1	-3.6	-0.7	---	---
Simple Law	Ship	1.5	1.4	0.6	2.1	4.1	8.4	19.3
	Buoy	-0.2	-1.0	0.0	-0.2	3.4	---	---
1000 mb	Ship	-0.7	-2.3	-1.3	-0.7	1.1	5.3	17.8
	Buoy	-2.1	-2.0	-2.1	-2.6	2.2	---	---
Yu	Ship	0.0	-2.5	-1.0	0.4	2.7	7.6	18.9
	Buoy	-1.8	-2.2	-1.8	-1.8	2.2	---	---
Cardone	Ship	2.1	-1.1	1.0	2.9	5.6	11.1	21.0
	Buoy	0.2	-0.8	0.2	0.5	5.3	---	---
Clarke/Hess	Ship	1.0	-2.0	0.0	1.7	4.4	8.7	20.1
	Buoy	-0.6	-1.7	-0.6	0.0	2.7	---	---
FNOC	Ship	0.5	-1.8	-0.2	1.0	2.8	7.0	17.3
	Buoy	-0.9	-1.2	-0.9	-1.1	1.9	---	---

Table 10. Ships/Buoys vs Models (analyses). Comparisons of Biases (algebraic differences) vs Various Wind Speeds (m/sec)

MODEL		RMS difference						
		0-45	0-5	5-10	10-15	15-22.5	22.5-30	30-45
Geostrophic	Ship	5.3	4.6	4.4	5.2	6.3	9.5	19.0
	Buoy	4.6	3.7	4.3	6.3	4.9	---	---
Simple Law	Ship	4.7	3,3	3.3	4.6	6.5	10.9	20.8
	Buoy	3.1	2.6	2.9	4.0	5.1	---	---
1000 mb	Ship	4.7	4.1	3.8	4.5	5.7	9.0	19.3
	Buoy	4.0	3.3	3.8	4.9	5.2	---	---
Yu	Ship	4.6	4.3	3.8	4.4	5.8	10.2	20.4
	Buoy	3.8	3.6	3.7	4.6	4.3	---	---
Cardone	Ship	5.1	3.0	3.3	4.9	7.3	12.7	21.9
	Buoy	3.2	2.4	2.9	4.4	6.4	---	---
Clarke/Hess	Ship	4.6	3.7	3.3	4.2	6.0	10.6	21.2
	Buoy	3.2	3.1	3.0	3.8	4.4	---	---
FNOC	Ship	4.3	3.6	3.4	4.0	5.6	9.5	19.4
	Buoy	3.2	2.6	2.9	4.5	4.1	---	---

Table 11. Ships/Buoys vs Models (analysis) Comparisons of RMS vs Various Wind Speeds.

The results of the study point out the difficulty of specifying and verifying winds over the oceans using boundary layer models with limited physics, reduced vertical resolution and lack of significant, accurate measurements at sea. The future lies in generating ocean surface wind fields using more complex boundary layer formulation schemes. At present the lowest layer in the NMC model is 11 mb thick and it is possible that future models will have even smaller thicknesses thereby possibly eliminating the need for special boundary layer models. The data issue will have to wait for satellite measurements to provide a comprehensive coverage of the global oceans.

REFERENCES

Burroughs, L. D., 1982. Coastal wind forecasts based on model output statistics. 9th Conference Weather Forecasting and Analysis Preprints, June 28 - July 1, 1986, Seattle, WA, pp 351-354.

Cardone,V.J. 1969.Specification of the wind field distribution in the marine boundary layer for wave forecasting. Report TR-69-1,Geophys. Sci.Lab., New York University. Available from NTIS AD#702-490.

Cardone, V. J. 1978. Specification and prediction of the vector wind one United States Continental shelf for applications to an oil slick trajectory forecast program. Final Report, Contract T-35430. The City College of the City University of New York.

Clark, L., 1986. Personal Communications, FNOC.

Clarke, R. H. and G. D. Hess, 1975. On the relation between surface wind and pressure gradient, especially in lower latitudes. Boundary Layer Meteorol. 9, pp 325-339.

Court, A. 1958. Wind correlation and regression. Sci. Report 3, Contract Af19(604)-2060. AFCRC, Hanscom Field, Bedford, Mass.

Dey, C. H. and L. L. Morone 1985. Evolution of the National Meteorological Center global data assimilation system: January 1982-December 1983, Mon. Wea. Rev., 113, pp 304-317.

Dischel, R. S. and W. J. Pierson 1986. Comparison of wind reports by ships and data buoys. Proceeding of the Marine Data Systems Symposium, Marine Technology Society, New Orleans, LA.

Earle, M. D. 1985. Statistical comparisons of ship and buoy data marine observations. Report MEC-85-8, MEC Systems Corporation, Manassas, Virginia

Gilhousen, D. B. 1986. An accuracy statement for meteorological measurements obtained from NDBC moored buoys. Proc. MDS, 1986. Marine Data Systems International Symposium, Marine Tech. Soc. April 30-May 2,1986, New Orleans, LA. pp 198-204.

Krishna, K., 1981. A two-layer first-order closure model for the study of the baroclinic atmospheric boundary layer. J. Atmosp. Sci., 38, pp 1401-1417.

Larson, S. E. 1975. A 26-year time series of monthly mean winds over the ocean, part 1. A statistical verification of computed surface winds over the North Pacific and North Atlantic. Tech. Paper No. 8-75, Envirn. Pred. Res. Fac., Naval Postgraduate School, Monterey, CA.

Mihok, W. F. and J. E. Kaitala, 1976. U. S. Navy Fleet Numerical Weather Central operational five-level global fourth-order primative-equation model, Mon. Wea. Rev, 104, pp. 1528-1550.

Miyakoda, K. and J. Sirutis, 1983. Manual of the E-Physics. Geophysical Fluid Dynamics Lab., NOAA. Princeton Univ., P. O. Box 308 Princeton, N. J., 03540.

National Climatic Data Center, 1983. Climatic summaries for NOAA data buoys. National Weather Service,NOAA, U.S. Department of Commerce, 214 pp.

Nicholls, S. and C. J. Reading 1979. Aircraft observations of the structure of the lower boundary layer over the sea, Quart. J. Roy. Meteorol. Soc., 105, pp. 785-802.

Sela, J. G. 1982. The NMC spectral model. NOAA Tech. Report NWS-30. U. S. Dept. of Commerce., NOAA, NWS.

Turner, D, B, 1986. Comparison of three methods for calculating the standard deviation of wind direction. J. Climate Appl. Meteorol., 25, pp 703-707.

Willmott, C. J. 1982. Some Comments on the Evaluation of Model Performance. Bull. Am. Meteorol. Soc., 63, pp 1309-1313.